A COMPOSITIONAL MODEL TO ASSESS EXPRESSION CHANGES FROM SINGLE-CELL RNA-SEQ DATA

XIUYU MA, AND CHRISTINA KENDZIORSKI, AND MICHAEL A. NEWTON

1. INTRODUCTION

The ability to measure genome-wide gene expression at single-cell resolution has accelerated the pace of biological discovery[1]. Overcoming data analysis challenges caused by the scale and unique variation properties of single-cell data will surely fuel further advances in immunology (cite), developmental biology (cite), and cancer (cite)(unsure about which paper to cite). Computational tools and statistical methodologies created for data of lower-resolution (e.g. bulk RNA-seq) or lower dimension (e.g. flow cytometry) guide our response to the data science demands of new measurement platforms, but they are not adequate for efficient knowledge discovery in this rapidly advancing domain[2].

An important feature of single-cell studies that could be leveraged better statistically is the fact that cells populate distinct, identifiable subtypes determined by lineage history, epigenetic state, the activity of various transcriptional programs (e.g. burst states), or other distinguishing factors. Lots of efforts have been made to clustering cells into different cell subtypes, SC3[3], CIDR[4] and ZIFA[5]. Whether or not a determination of cellular subtypes and their frequencies is a task of interest in a given application, we hypothesize that such subtype information may be injected into other inferences in order to improve their operating characteristics.

Assessing the magnitude and statistical significance of changes in gene expression associated with different cellular conditions has been a central statistical problem in genomics for which new tools specific to the single-cell RNAseq data structure have been deployed: MAST[6], DESEQ2[7], SCDD[8], etc. These tools respond to scRNAseq characteristics, such as high prevalence of zero counts and gene-level multimodality, but none takes explicit advanatage of cellular subtype information. We present a simple procedure and supporting theoretical analyses for this purpose. A notable technical innovation is a new prior distribution over pairs of multinomial probability vectors that conveys both marginal Dirichlet conjugacy as well as dependence induced through sharp equalities on aggregated subtype probabilities, which turns out to be key in formulating the posterior probability of changes in expression distributions between conditions.

In our compositional model, subtype that inferred from whole genome are fed into gene level expression. We utilize the mixture of subtypes to characterize transcripts profile and identify differential distributed genes across conditions in an scRNA-seq experiment. Simulation study suggests that the method provides improved power and precision for identifying differentially distributed genes. Performance on real data has been investigated through ten previously published experimental data from conquer[17]. We also obtained asymptotic properties of posterior inference.

2. Modeling

2.1. **Data structure, sampling model, and parameters.** In modeling scRNASeq data, we imagine that each cell falls into one of $K > 1$ classes, which we think of as subtypes or subpopulations of cells. Knowledge of this class structure prior to measurement is not required, as it will be inferred as necessary from available genomic data. We also assume that cells arise from multiple experimental conditions, such as by treatment-control status or some other factor measured at the cell level, and we present our development for the special case of two conditions. Let's say conditions 1 and 2 contain n_1 and n_2 cells, respectively, and let z_k^j denote the number of cells of subtype k in condition j. Count vectors $z^1 = (z_1^1, z_2^1, \cdots, z_K^1)$ and $z^2 = (z_1^2, z_2^2, \cdots, z_K^2)$ we treat as independent multinomial vectors, reflecting the common, two-condition experimental design. Explicitly,

$$z^1 \sim \text{Multinomial}_K(n_1, \phi) \quad \text{and} \quad z^2 \sim \text{Multinomial}_K(n_2, \psi)$$

for probability vectors $\phi = (\phi_1, \phi_2, \cdots, \phi_K)$ and $\psi = (\psi_1, \psi_2, \cdots, \psi_K)$ that characterize the populations of cells from which the $n_1 + n_2$ observed cells are sampled. As for data, the normalized expression of gene g in cell c, say $X_{g,c}$, is one entry in a typically large data matrix; and we record cell condition with the binary label y_c.

Our working hypothesis is that any differences in the distribution of $X_{g,c}$ between $y_c = 1$ and $y_c = 2$ (i.e., any condition effects) are attributable to differences between the conditions in the underlying composition of cell types; i.e., owing to $\phi \neq \psi$. We reckon that cells of any given subtype k will present data according to a distribution reflecting technical and biological variation specific to that class of cells, regardless of the condition the cell finds itself in. Some care is needed in this, as an overly broad cell subtype (e.g. *epithelial cells*) could have further subtypes that show differential response to some treatment, for example, and so cellular condition (treatment) would then affect the distribution of expression data within the subtype, which is contrary to our working hypothesis. On the other hand, we could then refine the subtype definition to allow more population classes K in order to mitigate that problem. We revisit the issue in discussion section, but for now proceed assuming that cellular condition affects the composition of subtypes but not the distribution of expression within a subtype.

With this working hypothesis, let $f_{g,k}(x)$ denote the sampling distribution of expression measurement $X_{g,c}$ assuming that cell c is from subtype k. Then in the two cellular conditions, the marginal distributions over subtypes are

$$f_g^1(x) = \sum_{k=1}^{K} \phi_k f_{g,k}(x) \quad \text{and} \quad f_g^2(x) = \sum_{k=1}^{K} \psi_k f_{g,k}(x).$$

We say that gene g is *differentially distributed*, denote DD_g, if $f_g^1(x) \neq f_g^2(x)$ for some x, and otherwise it is equivalently distributed (ED_g). Motivated by findings from bulk RNAseq data analysis, we further set each $f_{g,k}$ to have a a Negative Binomial form, say with mean $\mu_{g,k}$ and shape parameter α_g[16]. This choice proves to be effective in our numerical experiments though it is not critical to the modeling formulation.

We seek a useful methodology to prioritize genes for evidence of DD_g. Interestingly, even if we have evidence for condition effects on the subtype frequencies, it does not follow that a given gene will have $f_g^1 \neq f_g^2$; that depends on whether or not the subtypes show the right pattern of *differential expression* at g, to use the standard terminology from bulk RNAseq. For example, if two subtypes have different frequencies between the two conditions ($\phi_1 \neq \psi_1$ and $\phi_2 \neq \psi_2$) but the same aggregate frequency ($\phi_1 + \phi_2 = \psi_1 + \psi_2$), and also if $\mu_{g,1} = \mu_{g,2}$ then, other things being equal, $f_g^1 = f_g^2$ even though $\phi \neq \psi$. Simply, a gene that does not distinguish two subtypes will also not distinguish the cellular conditions if those subtypes appear in the same aggregate frequency in the two conditions, regardless of changes in the individual subtype frequencies. We formalize this idea in order that our methodology has the necessary functionality. First, consider the parameter space

$$\Theta = \{(\phi, \psi, \mu, \sigma)\}$$

where $\phi = (\phi_1, \phi_2, \cdots, \phi_K)$ and $\psi = (\psi_1, \psi_2, \cdots, \psi_K)$, as before, where $\mu = \{\mu_{g,k}\}$, all the subtype-and-gene-specific expected values, and where $\sigma = \{\sigma_g\}$ holds all the gene-specific Negative binomial shape parameters. We define special subsets of Θ using partitions of the K cell subtypes. A single partition, say π, is a set of mutually exclusive and exhaustive blocks, b, say, each a subset of $\{1, 2, \cdots, K\}$, and we write $\pi = \{b\}$. We recall that the set Π containing all partitions π of $\{1, 2, \cdots, K\}$ has cardinality that grows rapidly with K. We'll carry along an example involving $K = 7$ cell types, and one three-block partition taken from the set of 877 possible partitions of $\{1, 2, \cdots, 7\}$ (Figure 1).

For any partition $\pi = \{b\}$ we have aggregate subtype frequencies

$$\Phi_b = \sum_{k \in b} \phi_k \quad \text{and} \quad \Psi_b = \sum_{k \in b} \psi_k.$$

We'll also use the notation $\Phi_\pi = \{\Phi_b : b \in \pi\}$ and similarly for Ψ_π. As long as π is not the most refined partition, the mapping from (ϕ, ψ) to (Φ_π, Ψ_π) is many-to-one (Figure 1) Define

$$A_\pi = \{\theta \in \Theta : \Phi_b = \Psi_b \, \forall b \in \pi\}.$$
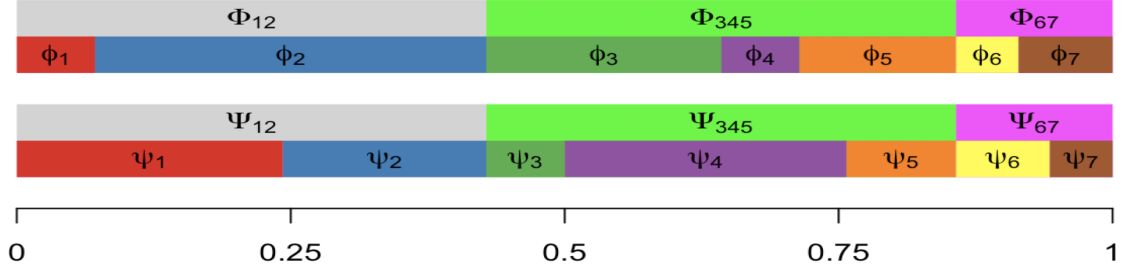
FIGURE 1. proportions of subtypes change in different conditions. Aggregated proportions of subtype 1 and 2, subtype 3, 4, 5, and subtype 6,7 remained same across conditions while proportion of individual subtype changed

and

$$M_{g,\pi} = \{\theta \in \Theta : \ \mu_{g,k} = \mu_{g,k'} \iff k, k' \in b, b \in \pi\}.$$

Indeed, these are precisely the structures needed to address differential distribution DD_g (and it complement, equivalent distribution, ED_g) at a given gene g:

Theorem 1. *Let $C_\pi = A_\pi \cap M_{g,\pi}$, for any different partitions π_1, π_2, $C_{\pi_1} \cap C_{\pi_2} = \emptyset$. At a given gene, equivalent distribution is*

$$ED_g = \bigcup_{\pi \in \Pi} C_\pi.$$

Our main purpose is to quantify probability of a gene being differentially distributed. Due to theorem 1 and independence between $M_{g,\pi}$ and A_π, we can achieve our purpose by separate estimations of $M_{g,\pi}$, which has been done in EBSeq[16], and A_π. In the following subsections we developed an empirical bayesian framework to quantify likelihood of A_π given estimated subtypes counts.

2.2. **Double Dirichlet prior.** Here we describe a prior $p(\phi, \psi)$ that is conjugate to multinomial sampling but that also enables downstream gene-specific inferences about differential distribution when certain cell types do not differ in their expression distributions.

For our purposes, the prior will have a spike-slab structure that mixes over distinct patterns of equality of π-associated accummulated probabilities:

$$p(\phi, \psi) = \sum_{\pi \in \Pi} P(A_\pi)\, p(\phi, \psi | A_\pi)$$

Unfortunately, we could not define the prior of (ϕ, ψ) on the whole space. Upon setting up a prior $p(\phi, \psi)$ that can mix over structures A_π, and by combining cell-type counts z^1 and

z^2 with expression data x_g at a gene, we may compute $P(\text{ED}_g|\text{data})$ at each gene:

$$
(1) \qquad P(\text{ED}_g|\text{data}) = \sum_{\pi \in \Pi} P(A_\pi|z^1, z^2)\, P(B_\pi|x_g).
$$

Initially, the multitude of $P(A_\pi)$'s will be preset constants. To complete the prior specification $p(\phi, \psi)$, consider further scalers $\alpha_k > 0$ for each class k and $\beta_b > 0$ for each potential block b. (Extending the notational convention, α_b is the vector of α_k for $k \in b$, and β_π is the vector of β_b for $b \in \pi$.) For any block b consider conditional probabilities

$$
\tilde{\phi}_b = \frac{\phi_b}{\Phi_b} \qquad \tilde{\psi}_b = \frac{\psi_b}{\Psi_b}
$$

which indicate the conditional probability of each class k given that the cell is of one of the types in b. Assume that conditional upon A_π,

$$
\Phi_\pi \sim \text{Dirichet}_{N(\pi)}[\beta_\pi]
$$

where $N(\pi)$ is the number of blocks b in π, and further that accumulated probabilities are the same between the two source conditions: $\Phi_\pi = \Psi_\pi$. Finally, assume that for each $b \in \pi$,

$$
\tilde{\phi}_b, \tilde{\psi}_b \sim_{\text{i.i.d.}} \text{Dirichlet}_{N(b)}[\alpha_b]
$$

where $N(b)$ is the number of cell types in block b. In other words, if A_π is the active structure, then accumulated probability vectors Φ_π and Ψ_π are equal between the two source conditions, though the sub-block class-specific rates ϕ_k and ψ_k may differ, as would (re-normalized) independent Dirichlet-distributed vectors. Taken together,

$$
p(\phi, \psi|A_\pi) = p(\Phi_\pi, \Psi_\pi|A_\pi) \prod_{b \in \pi} \left[p(\tilde{\phi}_b)p(\tilde{\psi}_b) \right]
$$

with

$$
p(\Phi_\pi, \Psi_\pi|A_\pi) = \frac{\Gamma(\sum_{b \in \pi} \beta_b)}{\prod_{b \in \pi} \Gamma(\beta_b)} \left[\prod_{b \in \pi} \Phi_b^{\beta_b - 1} \right] 1\left[\Phi_\pi = \Psi_\pi\right]
$$

and

$$
p(\tilde{\phi}_b) = \frac{\Gamma(\sum_{k \in b} \alpha_k)}{\prod_{k \in b} \Gamma(\alpha_k)} \prod_{k \in b} \tilde{\phi}_k^{\alpha_k - 1}, \qquad p(\tilde{\psi}_b) = \frac{\Gamma(\sum_{k \in b} \alpha_k)}{\prod_{k \in b} \Gamma(\alpha_k)} \prod_{k \in b} \tilde{\psi}_k^{\alpha_k - 1}.
$$

2.3. **Predictive and posterior probabilities:** For notation, we use ϕ_b for the vector of values ϕ_k for $k \in b$, and similarly for ψ_b. Analogously, Φ_π and Ψ_π are vectors of accumulated class probabilities ϕ_b and ψ_b for all $b \in \pi$, respectively.

In order to get the posterior probability $p(A_\pi|z^1, z^2)$, we need to calculate

$$p(A_\pi|z^1, z^2) \propto p(A_\pi, z^1, z^2) = \int_{A_\pi} p(z^1, z^2|\phi, \psi)p(\phi, \psi)d\phi d\psi$$

$$= \sum_{\pi' \in \Pi} \int_{A_\pi} p(z^1, z^2|\phi, \psi)p(\phi, \psi|A_{\pi'})p(A_{\pi'})d\phi d\psi$$

For simplicity of notation, let $w(\pi_1, \pi_2) = \int_{A_{\pi_1}} p(z^1, z^2|\phi, \psi)p(\phi, \psi|A_{\pi_2})p(A_{\pi_2})d\phi d\psi$, then $p(A_\pi|z^1, z^2) \propto \sum_{\pi' \in \Pi} w(\pi, \pi')$. To calculate component $w(\pi, \pi')$, recall refinement and coarseness relationship between partitions, we say a partition $\tilde{\pi}$ is a refinement of another partition π if $\forall b \in \pi$ there exists $s \subset \tilde{\pi}$ such that $\bigcup_{b' \in s} b' = b$. We say π is a coarseness of $\tilde{\pi}$ when $\tilde{\pi}$ refines π. we have following theorem

Theorem 2. *If π' is a refinement of π then $w(\pi, \pi') = w(\pi', \pi')$ otherwise $w(\pi, \pi') = 0$*

Consequently, let $RF(\pi)$ be the collection of finer partition of π, we have the posterior probability:

$$p(A_\pi|z^1, z^2) \propto \sum_{\pi' \in RF(\pi)} w(\pi', \pi')$$

Using the Dirichlet-Multinomial conjugacy and the collapsing property of these distributions ([11]), we get closed formulas for the predictive probability of cell-type counts z^1 and z^2. Fixing π, let $t_b^j = \sum_{k \in b} z_k^j$, for cell conditions $j = 1, 2$, record the total numbers of cells accumulated over all types in block b. And following our notation convention, t_π^j is the vector of these counts over $b \in \pi$. From the prior and model structure

$$w(\pi', \pi') = p(z^1|t_{\pi'}^1)\, p(z^2|t_{\pi'}^2)\, p(t_{\pi'}^1, t_{\pi'}^2|A_{\pi'})p(A_{\pi'}).$$

Conditional independence of z^1 and z^2 given the block-level totals $t_{\pi'}^1$ and $t_{\pi'}^2$ on $A_{\pi'}$ reflects the possible differential class proportion structure within blocks but between cell conditions. For either cellular group $j = 1, 2$, we find, after some simplification, the following Dirichlet-Multinomial masses:

$$(2) \qquad p(z^j|t_{\pi'}^j) = \prod_{b \in \pi'} \left\{ \left[\frac{\Gamma(t_b^j + 1)}{\prod_{k \in b} \Gamma(z_k^j + 1)} \right] \left[\frac{\Gamma(\sum_{k \in b} \alpha_k)}{\prod_{k \in b} \Gamma(\alpha_k)} \right] \left[\frac{\prod_{k \in b} \Gamma(\alpha_k + z_k^j)}{\Gamma(t_b^j + \sum_{k \in b} \alpha_k))} \right] \right\}$$

and

(3)

$$p(t_{\pi'}^1, t_{\pi'}^2|A_{\pi'}) = \left[\frac{\Gamma(n_1 + 1)\Gamma(n_2 + 1)}{\prod_{b \in \pi'} \Gamma(t_b^1 + 1)\Gamma(t_b^2 + 1)} \right] \left[\frac{\Gamma(\sum_{b \in \pi'} \beta_b)}{\prod_{b \in \pi'} \Gamma(\beta_b)} \right] \left[\frac{\prod_{b \in \pi'} \Gamma(\beta_b + t_b^1 + t_b^2)}{\Gamma(n_1 + n_2 + \sum_{b \in \pi'} \beta_b)} \right].$$

Let's look at some special cases to dissect this result.

Case 1. If π' has a single block equal to the entire set of cell types $\{1, 2, \cdots, K\}$, then

$t_b^j = n_j$ for both $j = 1, 2$, and the second formula reduces, correctly, to $p(t_{\pi'}^1, t_{\pi'}^2 | A_{\pi'}) = 1$. Further,

$$p(z^j | t_{\pi'}^j) = \left[\frac{\Gamma(n_j + 1)}{\Gamma(n_1 + \sum_{k=1}^K \alpha_k)} \right] \left[\frac{\Gamma(\sum_{k=1}^K \alpha_k)}{\prod_{k=1}^K \Gamma(\alpha_k)} \right] \left[\prod_{k=1}^K \frac{\Gamma(\alpha_k + z_k^j)}{\Gamma(z_k^j + 1)} \right]$$

which is the well-known Dirichlet-multinomial predictive distribution for counts z^j [12]. E.g, taking $\alpha_k = 1$ for all types k we get the uniform distribution

$$p(z^j | t_{\pi'}^j) = \frac{\Gamma(n_j + 1)\Gamma(K)}{\Gamma(n_j + K)}.$$

Case 2. At the opposite extreme, π' has one block b for each class k. Then $t_b^j = z_k^j$, and $p(z^j | t_{\pi'}^j) = 1$, and further, assuming $\beta_b = \alpha_k$,

$$p(t_{\pi'}^1, t_{\pi'}^2 | A_{\pi'}) = \left[\frac{\Gamma(n_1 + 1)\Gamma(n_2 + 1)}{\prod_{k=1}^K \Gamma(z_k^1 + 1)\Gamma(z_k^2 + 1)} \right] \left[\frac{\Gamma(\sum_{k=1}^K \alpha_k)}{\prod_{k=1}^K \Gamma(\alpha_k)} \right] \left[\frac{\prod_{k=1}^K \Gamma(\alpha_k + z_k^1 + z_k^2)}{\Gamma(n_1 + n_2 + \alpha_k)} \right].$$

which corresponds to Dirichlet-multinomial predictive distribution for counts $z^1 + z^2$ since z^1 and z^2 are identical distributed in this case.

Regardless of the partition, log scale probabilities are readily evaluated given hyper-parameters $\{\alpha_k\}$ and $\{\beta_b\}$ and for cell-type counts z^1 and z^2.
For asymptotic properties of the posterior probabilities, we demonstrated them in section 5.

3. Data analysis workflow

3.1. **Basic workflow.**

Algorithm 1

    Input: normalized transcripts profile from two conditions X_1, X_2
    Output: posterior probabilities of genes being differential distributed
1: **procedure** SCDDBOOST(X_1, X_2)
2:     $Z \leftarrow$ identify subtypes of pooled cells(X_1, X_2)
3:     $P(M_{g,\pi} | X_1, X_2) \leftarrow$ EBSeq[16]
4:     $P(A_\pi | Z) \leftarrow$ Empirical Bayes via double dirichlet prior
5:     $P(\text{ED}_g | X_1, X_2) \leftarrow \sum_\pi P(M_{g,\pi} | X_1, X_2) P(A_\pi | Z)$
6:     $P(\text{DD}_g | X_1, X_2) \leftarrow 1 - P(\text{ED}_g | X_1, X_2)$
7:     **return** $P(\text{DD}_g | X_1, X_2)$

In our basic workflow, the input are transcripts processed by normalizing methods (e.g. SCnorm [15]). Prior to any bayesian inference, we need to identify subtypes of cells. One advantage of our approach is that the posterior inference can be incorporate with different

clustering methods. The essential idea is that the mixture structure is estimated using the whole genome information rather than at each gene solely using information of that gene to estimate a gene specific mixture structure. Due to this reason, our model is more capable of capturing characteristic of scRNA seq data than scDD and we name our approach scDDboost.

There are many single cell clustering methods(e.g. SC3[3], CIDR[4] and ZIFA[5]) that could utilized in the workflow. However, for the integrity of our work and speeding in computation, we present another efficient and effective clustering procedure. We pool cells from two conditions. At each gene level, we do a Poisson-Gamma model extended from modal clustering[9]. After gene level clustering, we use the cluster-based similarity partition algorithm (CSPA[10]). For each individual clustering result, a binary similarity matrix is constructed from the corresponding cell labels: if two cells belong to the same cluster, their similarity is 1; otherwise their similarity is 0. We obtain a consensus similarity matrix M_1 by averaging all similarity matrices of individual clusterings. Another distance matrix M_2 calculated by Pearson distance between cells. A final similarity matrix is obtained by weighted combining M_1 and M_2. Cells are classified into subtypes by K-medoids based on the final similarity matrix.

After identification of subtypes, the following two steps use empirical Bayes to provide posterior inference on patterns of differential expression and aggregated proportions of subtypes, which are components of posterior probabilities for a gene being equivalent distributed. Combining those components, final posterior probabilities are obtained.

3.2. **Simulation study.**
A simulation study was conducted to assess the performance of scDDboost in identifying DD genes. We simulate data by splatter[14] with approximate 200 cells each condition and 7 subtypes with proportions ϕ and ψ from Figure 1 satisfying constraints: $\phi_1+\phi_2 = \psi_1+\psi_2$, $\phi_3 + \phi_4 + \phi_5 = \psi_3 + \psi_4 + \psi_5$ and $\phi_6 + \phi_7 = \psi_6 + \psi_7$. Each subtype has 10% genes to be differential expressed. We view the differences among subtypes by projecting transcripts profiles of cells into its first two principal components(figure 3). We observed subtypes are well separated, which is driven by genes with heterogeneous distribution between subtypes.

We determine the number of subtypes by searching a range of candidates(from 1 to 9 based on our empirical experience). Given number of subtypes, we obtain a subtype structure of cells, which will further be fed into computing the posterior probabilities. We visualize the change between posterior probabilities under number of clusters i and $i+1$(i from 1 to 8). It typically remains stable when number of cluster is above a number that is smaller than 9 (figure 4) In the simulated data, the posterior probability become stable when we overestimate the number of subtypes. We found the true number of subtypes is 7 and correctly identify the subtypes of cells.
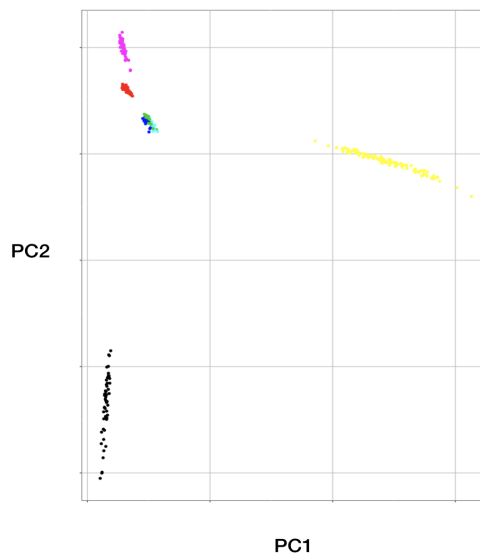
FIGURE 2. first two principal components of transcripts, which demonstrates the difference between subtypes. Even if we projected transcripts of cells into two dimensional space, we observe subtypes are well separated.

10% DE genes in each subtype results in total 9067 DD genes and 8306 ED genes in the mixture of the 7 subtypes. Table 1 are numbers of DD or DE genes identified by four methods (scDDboost, scDD, MAST and DESeq2) with target FDR at 5 %.

	scDDboost	scDD	MAST	DESeq2
DD or DE genes	6073	3038	2468	2076
True positive	4774	2724	2442	2073
false positive	1299	314	26	3

TABLE 1. number of true positive and false positive genes identified by four methods. Target FDR at 5%

scDDboost identified most true DD genes, the reason is that mean expression shifts between conditions is not as significant as mean expression shifts between subtypes, which limits the power of MAST and DESeq2. Our approach and scDD considered mixture structure underlying the transcrips but scDD did not use the whole genome information to infer mixture components, which leads to inaccurate clustering at gene level and reduce the power. scDDboost could correctly identify the subtypes of cells and thus are more sensitive to the mean expression change among subtypes. We also compare roc curves of scDDboost, scDD, MAST and DESeq2. (figure 5)
Since we are modeling gene transcript within each subtype as negative binomial distributed and we only test one parameter(mean) change among subtypes. In some situation, it could
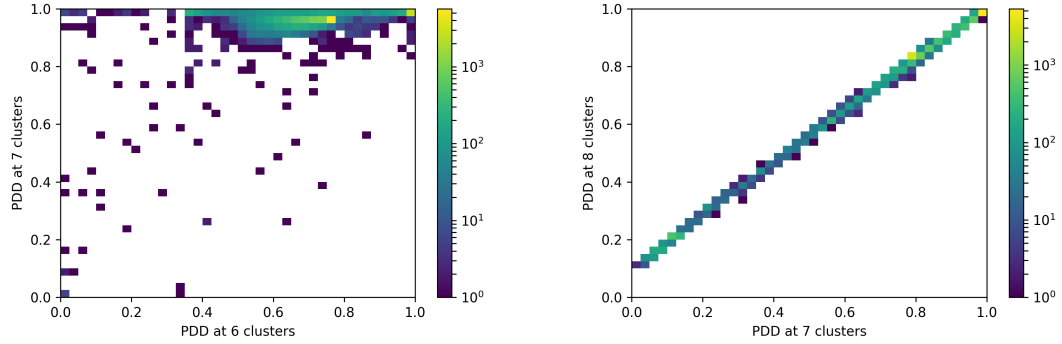
FIGURE 3. comparison of posterior probabilities of being DD among different number of subtypes, when we underestimate the number of subtypes, the difference is huge, see PDD between 6 subtypes and 7 subtypes. When we overestimate the number of subtypes, though inflating PDD (intercept is greater than 0 in the right panel) but the variation of difference is small, we observe a linear relation between PDD of 7 subtypes and 8 subtypes
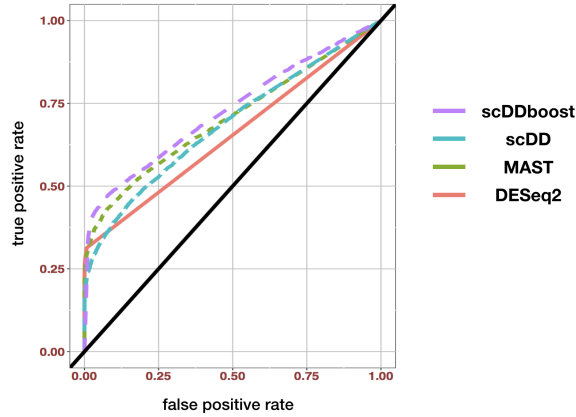

FIGURE 4. Roc curve of scDDboost, scDD, MAST and DESeq2, scDDboost has largest area under the roc curve. Roc curves of Mast and scDD are similar. For those roc curve there is bigger difference at low level of false positive rate, as scDDboost identified twice many true DD genes as other methods.

be insufficient for modeling the variability within subtype. Even though there is no mean expression change among subtypes but the distribution among subtypes changed, EBSeq would fail to detect the discrepancies between subtypes, thus reduce power of detecting

DD genes.

4. Examples

We use ten datasets from conquer[17] to test performance of our method on real data. We compare our results with scDD[8], MAST[6] and DESeq2[7]

Data set	Compared cell subsets	Number of cells per condition	Organism	Ref
GSE45719	16-cell stage blastomere vs Mid blastocyst cell (92-94h post- fertilization)	50, 60	mouse	[18]
GSE45719null	16-cell stage blastomere	50	mouse	[18]
GSE48968-GPL13112	BMDC (1h LPS stimulation) vs BMDC(4h LPS stimulation)	96, 95	mouse	[19]
GSE48968-GPL13112null	BMDC (1h LPS stimulation)	96	mouse	[19]
GSE60749-GPL13112	v6.5 mouse embryonic stem cells, culture conditions: 2i+LIF vs v6.5 mouse embryonic stem cells, culture conditions: serum+LIF	90, 94	mouse	[20]
GSE60749-GPL13112null	v6.5 mouse embryonic stem cells, culture conditions: 2i+LIF	90	mouse	[20]
GSE74596	NKT0 vs NKT17	45,44	mouse	[21]
GSE74596null	NKT0	45	mouse	[21]
EMTAB2805	G1 vs G2M	96,96	mouse	[22]
EMTAB2805null	G1	96	mouse	[22]
GSE63818-GPL16791	Primordial Germ Cells, developmental stage: 7 week gestation vs Somatic Cells, developmental stage: 7 week gestation	39,26	mouse	[23]
GSE71585-GPL13112	Chrna2 tdTpositive vs Cux2 tdTpositive	84, 124	mouse	[24]
GSE71585-GPL13112null	Chrna2 tdTpositive	84	mouse	[24]
GSE75748	NPC vs DEC	64, 87	human	[25]
GSE75748	NPC	64	human	[25]
GSE75748	DEC vs EC	70, 64	human	[25]
GSE75748	DEC	70	human	[25]
GSE64016null	H1 exp1 vs H1 exp2	64, 87	human	[26]

TABLE 2. single cell transcripts profiles used for differential expression or distribution method evaluation

We have table of numbers of differentially expressed genes of each dataset by MAST and DESeq2, and numbers of differentially distributed genes of each dataset by scDDboost and scDD.

Data set	scDDboost	scDDboost-sc3	scDD	MAST	DESeq2	total number of genes
GSE45719	5758	4228	6416	5652	11202	45686
GSE48969-GPL13112	11691	9819	2080	3396	9542	45686
GSE60749-GPL13112	19215	19168	18074	13674	23178	45686
GSE74596	1942	1353	1099	540	3796	45686
EMTAB 2805	5295	3748	2202	1088	5391	45686
GSE63818-GPL16791	3948	3480	1365	873	8934	45686
GSE71585-GPL13112	2902	1460	1622	2572	7378	24057
NPC-DEC	4377	3211	5982	6666	8439	19037
DEC-EC	3402	3023	3818	5429	8127	19037
H1 exp1-H1 exp2	0	0	1300	2077	2841	16579

TABLE 3. number of genes detected as significantly DE or DD

We found that bulk method DESeq2 tends to have the most number of DE genes. But among single cell methods we found that scDDboost usually had the most number of DD genes. Further we observed quite a few genes uniquely identified by scDDboost are likely to have different distribution across conditions. For example, figure 6, we use violin plot to demonstrate the log expression profiles among DEC and EC.

Although bulk methods seems to be the most powerful one, we found it also has a higher false discovery rate comparing to single cell methods. We validate false discovery rate on ten null datasets from table 1. For each null dataset, we randomly split the cells from one condition into two equal sized subsets and do DE analysis between those subsets. Since those two subsets of cells actually came from same condition, there should not be any differential distributed genes, any positive call would be a false positive. We repeat the random split and testing for five times on each null data set. We evaluate the type I error control for the methods returning nominal p-values, by recording the fraction of genes(with
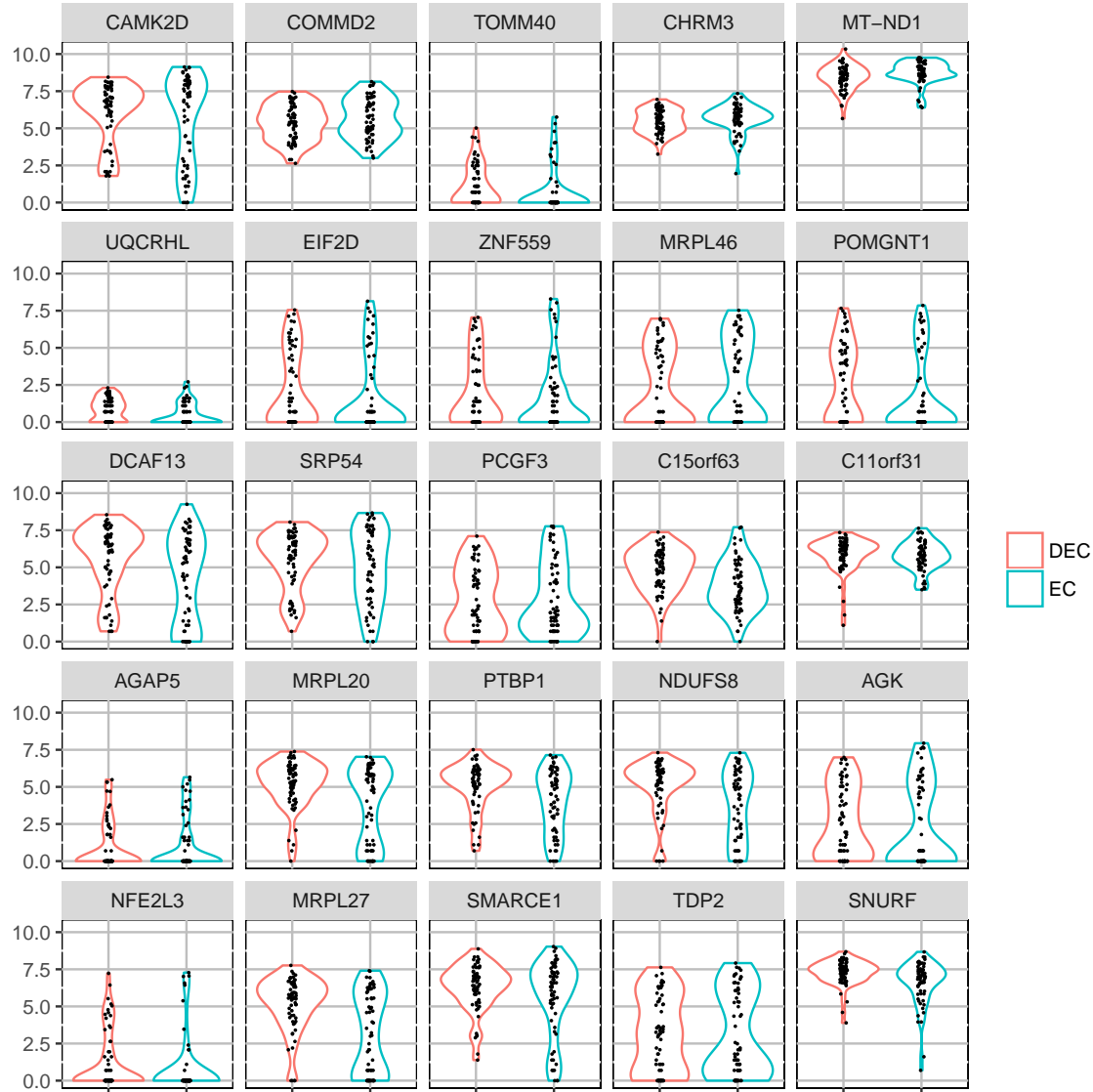
FIGURE 5. Densities of log transformed transcripts 25 DD genes uniquely identified by scDDboost, for data GSE75748, DEC vs. EC, We observe some of the genes are different distributed across conditions. *** may need other plot to further investigate those genes that are appear to be DE but identified as DD***

a valid p-value) that are assigned a nomial p-value below 0.05 (figure 5).
scDDboost could control FDR since we assume cells are sampled from population composed

of different subtypes. Cells from one subtype are equal likely to be assigned to either one of the two subsets. Consequently, proportions of subtypes remain unchanged among the two subsets.
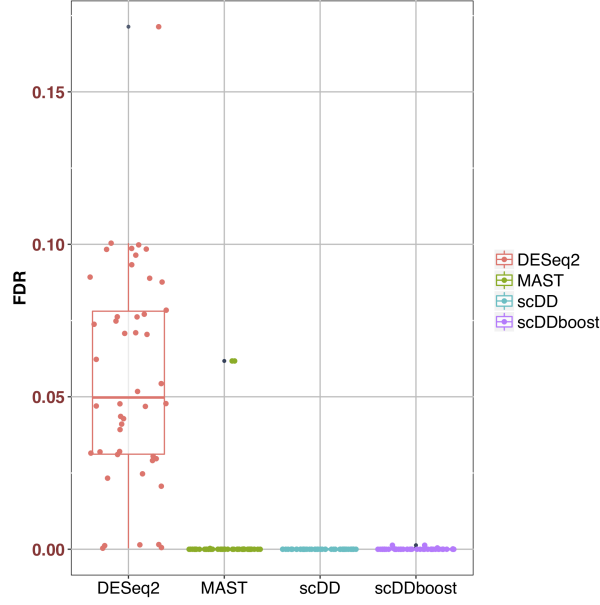
FIGURE 6. FDR of scDDboost, scDD, MAST and DESeq2 on null dataset from table 1, DESeq2 usually identify a lot but may lose the control of type I error. While other single cell methods could control FDR. ***This procedure for testing FDR, we randomly split a population into two samples, so it is highly likely proportion of subtypes remain same among these two samples, scDDboost always give small PDD and almost make no false positive call. This is kind different from really examining the FDR of scD-Dboost, where we have different proportions across conditions, but we do not want false call on those genes without mean expression change even there is proportion change. In this case, it actually reduce to the FDR of EBSeq whether we make correct posterior inference on DE pattern. The test of proportion is only done once, so scDDboost could still control FDR***

D3E[27] is a distributional method that can identify bursting parameters of transcripts. Rate of promoter activation, rate of promoter inactivation and the rate of transcription when the promoter is in the active state are estimated by D3E. We investigate DD genes identified by scDDboost and their change of those three parameters on dataset EMTAB2805
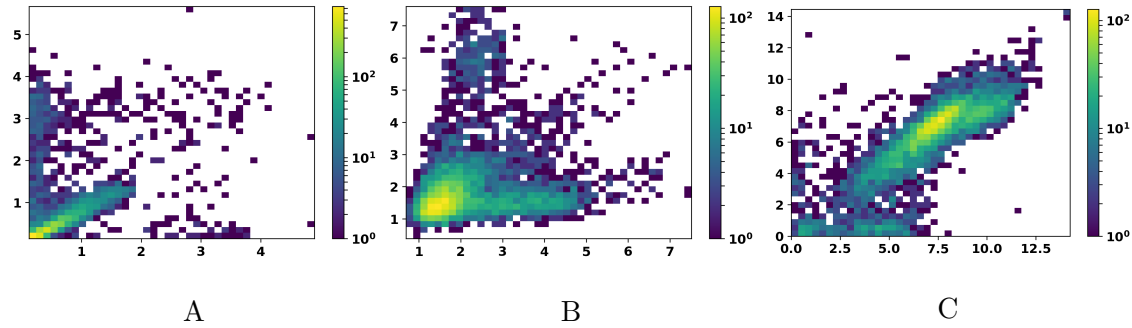
FIGURE 10. 2D histogram for bursting parameters of DD genes identified by scDDboost from dataset EMTAB2805 estimated by D3E. Panel A : comparison of rate of promoter activation between two conditions, similarly, panel B : rate of promoter inactivation and panel C : rate of transcription when the promoter is in the active state. We observe that difference between transcription rate is smaller compare to difference between the activation and inactivation rate. ***other methods also observe similar phenomena, this is not unique to scDDboost, main reason is that estimation from D3E tends to give larger difference in activation and inactivation rate than transcription rate. We may argue the major factor to drive DD genes are activation and inactivation rate (proportions of different subtyps), so it make sense to consider mixture model like scDDboost.***

We observed that DD genes identified by scDDboost tends to have similar transcription rate when the promoter is active across condition, while there are lots of variabilities in the action and inactivation rate. These results reveal that DD genes identified by scDDboost are driven by the change of activation and inactivation rates.

5. ASYMPTOTIC PROPERTIES

To investigate asymptotic properties we first give the expression of posterior probability. Since there is no information favorable of any particular A_π, we select discrete uniform distribution as the prior for it, then the posterior probability is

$$(4) \qquad p(A_\pi | z^1, z^2) = c * \sum_{\pi' \text{ refines } \pi} p(z^1 | t^1_{\pi'}) \, p(z^2 | t^2_{\pi'}) \, p(t^1_{\pi'}, t^2_{\pi'} | A_{\pi'})$$

for a normalizing constant $\frac{1}{c} = \sum_{\pi' \in \Pi} p(z^1 | t^1_{\pi'}) \, p(z^2 | t^2_{\pi'}) \, p(t^1_{\pi'}, t^2_{\pi'} | A_{\pi'})$.

There is a subset of Ω we lack posterior inference. Let us first see an example:

In figure 2, there are four subtypes, the rectangle with magenta boundary is a simplex $A_{\pi_1} = \{(\phi, \psi) : \phi_1 + \phi_2 = \psi_1 + \psi_2\}$, the rectangle with blue boundary is a simplex $A_{\pi_2} =$
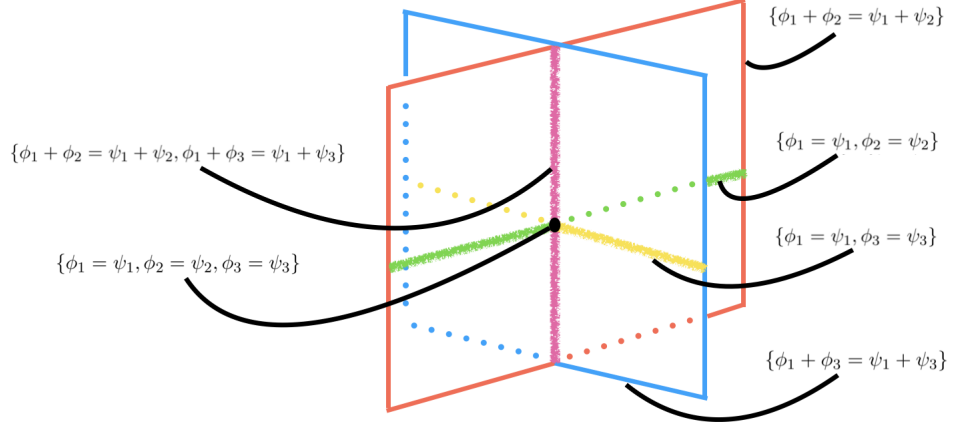
FIGURE 11. Four subtypes of cells, simplexes of (ϕ, ψ) satisfying different constraints.

$\{(\phi, \psi) : \phi_1 + \phi_3 = \psi_1 + \psi_3\}$. The green line refers to $A_{\pi_3} = \{(\phi, \psi) : \phi_1 = \psi_1, \phi_2 = \psi_2\}$, the yellow line refers to $A_{\pi_4} = \{(\phi, \psi) : \phi_1 = \psi_1, \phi_3 = \psi_3\}$, the purple line refers to $A_{\pi_5} = \{(\phi, \psi) : \phi_1 + \phi_2 = \psi_1 + \psi_2, \phi_1 + \phi_3 = \psi_1 + \psi_3\}$, which is the intersection of A_{π_1} and A_{π_2}, and finally the black dot which is the intersection of those three lines refers to the simplex with finest partitions, $\phi_i = \psi_i, \forall i = 1, .., 4$. We lack posterior inference for (ϕ, ψ) along the purple line except the black dot. While on the green line, yellow line and black dot, we have consistent posterior inference(theorem 2). To explain why some space lacking posterior inference and define such space, we define a special subset A_π^* of simplex A_π. $A_\pi^* = A_\pi \setminus \underset{\tilde{\pi} \text{ is not coarser than } \pi}{\cup} A_{\tilde{\pi}}$, A_π^* is obtained by removing all intersection with other $A_{\tilde{\pi}}$(excluding those $A_{\tilde{\pi}}$ that is superset of A_π) from A_π. Since we removed those intersection parts. It is intuitive that A_π^* will be disjoint subsets of Ω.

Proposition 1. *if $\pi_1 \neq \pi_2$, then $A_{\pi_1}^* \cap A_{\pi_2}^* = \emptyset$*

Let $Q = \Omega \setminus \underset{\pi \in \Pi}{\cup} A_\pi^*$, first thing to check is whether Q exists.

Proposition 2. *Let K be number of subtypes. When $K > 3, Q \neq \emptyset$, when $K \leq 3, Q = \emptyset$*

When number of subtypes bigger than three, we lack posterior inference on Q. To see

that we can rewrite A_π^* as $A_\pi^* = A_\pi \setminus \bigcup_{\tilde{\pi} \text{ is not coarser than } \pi} (A_{\tilde{\pi}} \cap A_\pi)$, $\tilde{\pi}$ is not coarser than π, which is equivalently to say π is not refinement of $\tilde{\pi}$. By lemma 1, $A_{\tilde{\pi}} \cap A_\pi$ is a lower dimensional subset of A_π. So $A_\pi \setminus A_\pi^*$ is a lower dimensional subset of A_π. For posterior on Q, it degenerates to integral on a lower dimensional subset of the simplex associating with densities, which will vanish

Proposition 3. *When $K > 3$, $p(Q|z^1, z^2) = 0$*

But for $(\phi, \psi) \in \Omega \setminus Q$, we have consistent posterior inference. Assuming $\alpha_i = 1, \forall i$ in (2) and $\beta_b = \Sigma_{i \in b} \alpha_i$ in (3), plug in (4) then we have simplified

$$(5) \qquad p(A_\pi | z^1, z^2) = \frac{1}{c'} \sum_{\pi' \in \mathrm{RF}(\pi)} \prod_{b \in \pi'} \frac{\Gamma(\beta_b + t_b^1 + t_b^2)}{\Gamma(\beta_b + t_b^1)\Gamma(\beta_b + t_b^2)}$$

$c' = c/\frac{\Gamma(n+1)\Gamma(n+1)\Gamma(K)}{\Gamma(2n+K)}$ And we have theorem 2.

Theorem 3. *Let $n = min(n_1, n_2)$ be the smaller number of cells of two conditions and $n_1 = O(n_2)$, when parameter $(\phi, \psi) \in \Omega \setminus Q$ we have*

$$p(A_\pi | z^1, z^2) \xrightarrow[n \to \infty]{a.s.} \begin{cases} 1 & if \ (\phi, \psi) \in A_\pi \\ 0 & otherwise \end{cases}$$

Things become more complicate when (ϕ, ψ) falling into Q, we know $p(Q|z^1, z^2) = 0$, but $p(A_\pi|z^1, z^2)$ may not vanish even the sample size is sufficiently large. Recall $N(\pi)$ represents number of blocks b in π. Let $S = \{\pi, (\phi, \psi) \in A_\pi\}$, which is the collection of partitions whose associated simplexes covering (ϕ, ψ). Let $N^* = \max_{\pi \in S} N(\pi)$, which is the max number of blocks of partitions from S. Let $S^* = \{\pi, (\phi, \psi) \in A_\pi \text{ and } N(\pi) = N^*\}$, which is the collection of partitions that covering (ϕ, ψ) with number of blocks equal to the max number N^*. For example, when $K = 7$, For a $(\phi, \psi) \in A_{\pi_1} \cap A_{\pi_2} \cap A_{\pi_3}$, $\pi_1 = \{\{1, 2, 3\}, \{4, 5, 6, 7\}\}, \pi_2 = \{\{1, 6, 7\}, \{2, 4\}, \{3, 5\}\}, \pi_3 = \{\{1, 2, 3, 4, 5, 6\}\}$, and also (ϕ, ψ) does not belong to any other simplex A_π. Then $S = \{\pi_1, \pi_2, \pi_3\}, N^* = 3, S^* = \{\pi_2\}$. Denote components from right hand side of (5): $\frac{1}{c'} \prod_{b \in \pi} \frac{\Gamma(\beta_b + t_b^1 + t_b^2)}{\Gamma(\beta_b + t_b^1)\Gamma(\beta_b + t_b^2)} = J(z^1, z^2, \pi)$. We have theorem 3.

Theorem 4. *Following the setting in theorem 2, when parameter $(\phi, \psi) \in Q$, and we have*

$$J(z^1, z^2, \pi) \xrightarrow[n \to \infty]{a.s.} \begin{cases} m(\pi) & \pi \in S^* \\ 0 & otherwise \end{cases}$$

and $\sum_{\pi \in S^*} m(\pi) = 1, m(\pi) > 0$

proofs are in the appendix.

Still using above example, in limiting case, we have $p(A_{\pi_3}|z^1, z^2) = 1$, $p(A_{\pi_2}|z^1, z^2) = 1$ and $p(A_{\pi_1}|z^1, z^2) = 0$. When the DE pattern is B_{π_1} for some genes. Since our underestimation of $p(A_{\pi_1}|z^1, z^2) = 0$, we will falsely classify those genes as differential distributed.

The asymptotic properties help us gain insight of the performance of our approach, scDDboost may work poorly, when $(\phi, \psi) \in Q$, we may underestimate the posterior probability of true proportion change pattern, which reduce the posterior probabilities of true negative and enlarge false positive rate.

6. Discussion

Cluster cells is an unsupervised learning, we do not know the true underlying partition and different number of clusters will lead to large differences in posterior probabilities of genes being differentially distributed (figure 7). We propose a modified bootstrap to stabilize our inferences. Instead of resample the cells, we resample the distance matrices of cells by adding noises to original distance matrix. Denote the original distance matrix as $D = (d_{i,j})$, for each time we random sample a vector e with length equal to number of cells and components are i.i.d. exponentially distributed. let w be the standard deviation of $d_{i,j}$. We resample a new $\hat{D}$ by adding nosies: $\hat{d}_{i,j} = d_{i,j} + e_i * w + e_j * w$. For $\hat{D}$ we still have triangle inequality held as $\hat{d}_{i,j} + \hat{d}_{j,k} \geq \hat{d}_{i,k}$, it is a valid distance matrix. For a fixed number of clusters, we average posterior probabilities over different distance matrices. And we select number of clusters K that posterior probabilities do not vary too much under K and $K+1$. From our empirical experience, it is typical K will not be larger than 8.
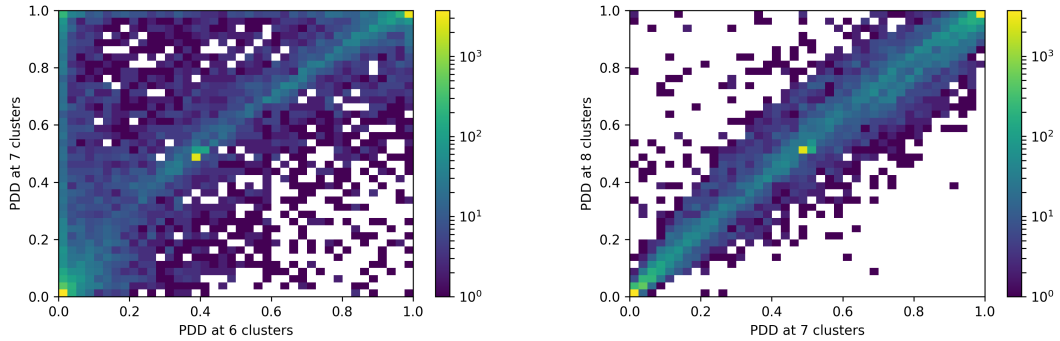

FIGURE 12. selecting number of subtypes for data GSE75748, we observe posterior probabilities become stable at more than 6 subtypes. Since increasing number of subtypes tends to decrease sample size of each subtypes, make complicate constraints for equivalent distribution and inflate estimated PDD. We select number of subtypes to be 7
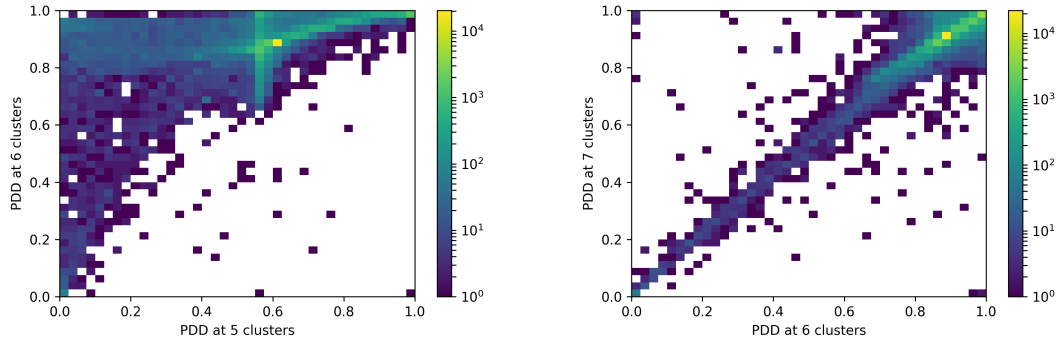
FIGURE 13. selecting number of subtypes for data GSE48968, we observe posterior probabilities become stable at more than 5 subtypes

Appendix A

Lemma 1. *If π_2 is not refinement of π_1 then $A_{\pi_1} \cap A_{\pi_2}$ is a lower dimensional subset of A_{π_2}*

Proof of theorem 2

$$w(\pi, \pi') = \int_{A_\pi \cap A_{\pi'}} p(z^1, z^2 | \phi, \psi) p(\phi, \psi | A_{\pi'}) p(A_{\pi'}) d\phi d\psi$$

where $p(z^1, z^2 | \phi, \psi) = p(z^1 | \phi) p(z^1 | \psi)$, $z^1 | \phi \sim$ multinomial$(n_1, \phi), z^2 | \psi \sim$ multinomial(n_2, ψ). Recall the definition of $A_\pi = \{(\phi, \psi) : \Phi_b = \Psi_b\}$ and A_π is a simplex. Denote the finest partition as $\pi_F = \{\{1\}, \{2\}, ..., \{K\}\}$, associated simplex $A_{\pi_F} = \{(\phi, \psi) : \phi_i = \psi_i, i = 1, ..., K\}$ for any two partition π_1 and π_2, intersection of their associated simplex must not be empty since $A_{\pi_F} \subset A_{\pi_1} \cap A_{\pi_2} \neq \emptyset$. To discuss the issue of overlapping of simplex A_π, we first introduce some notations. The whole space $\Omega = \{(\phi, \psi), \phi_i, \psi_i > 0$ and $\sum_{i=1}^K \phi_i = \sum_{i=1}^K \psi_i = 1\}$ and we define the refinement and coarseness relationship between partitions, we say a partition $\tilde{\pi}$ refines another partition π if $\forall b \in \pi$ there exists $s \subset \tilde{\pi}$ such that $\cup_{b' \in s} b' = b$. When $\tilde{\pi}$ refines π, we say $\tilde{\pi}$ is a refinement of(finer than) π or π is a coarseness of(coarser than) $\tilde{\pi}$. Observe that if π' refines π, then $A_\pi \cap A_{\pi'} = A_{\pi'}$, $\int_{A_\pi \cap A_{\pi'}} p(z^1, z^2 | \phi, \psi) p(\phi, \psi | A_{\pi'}) d\phi d\psi = \int_{A_{\pi'}} p(z^1, z^2 | \phi, \psi) p(\phi, \psi | A_{\pi'}) d\phi d\psi$. When π' is not refinement of π, we need to know the dimension of $A_\pi \cap A_{\pi'}$. Consider a map $f : b \to v$, which maps the block b to a vector $v \in \{0, 1\}^K$, the ith component of v is $1_{\{i \in b\}}$. And denote dim(S) be the dimension of space S. A_π can be equivalently defined as $A_\pi = \{(\phi, \psi) : M_\pi * (\phi - \psi) = 0\}$, M_π is a matrix with rows be $v_b = f(b), \forall b \in \pi$, that is to say (ϕ, ψ) are in the null space of linear transformation M_π. We have following lemma

Proof. Let V denote the orthogonal space of $\phi - \psi$, when $(\phi, \psi) \in A_{\pi_1} \cap A_{\pi_2}$, and dim$(A_{\pi_1} \cap A_{\pi_2}) = $ dim$(\phi - \psi) + $ dim$(\psi) = 2K - $ dim$(V) - 1$. Also let $\pi_1 = \{b_1^1, ..., b_s^1\}, \pi_2 = \{b_1^2, ..., b_t^2\}$. The corresponding vectors are $v_1^1, ..., v_s^1$ and $v_1^2, ..., v_t^2$. We claim there must be a $b_i^1 \in \pi$ whose corresponding v_i^1 is linear independent with $v_1^2, ..., v_t^2$. If not, for every v_i^1 there exists $\alpha_1^i, ..., \alpha_t^i$ such that

$$v_i^1 = \sum_{j=1}^t \alpha_j^i v_j^2 \qquad (*)$$

If $b_j^2 \cap b_i^1 \neq \emptyset$, then multiply v_j^2 on both sides of (*), we obtain $v_i^1 * v_j^2 = \alpha_j^i (v_j^2)^2$, as v_j^2 are orthogonal vectors, and $v_i^1 * v_j^2 > 0$ implies $\alpha_j^i > 0$. Consider $x = f(b_j^2 \setminus b_i^1)$, we have $x * v_i^1 = 0$ and we multiply x on both sides of (*) to obtain $\alpha_j^i v_j^2 * x = 0$, thus x must be zero vector and $b_j^2 \setminus b_i^1 = \emptyset$, which implies $b_j^2 \subset b_i^1$. That is to say when $b_j^2 \cap b_i^1 \neq \emptyset$, b_j^2 must be subset of b_i^1. So b_i^1 is union of some blocks in π_2. Which implies π_2 is refinement of π_1,

contradiction.

Consequently there exists $b \in \pi_1$ with $v(b)$ linear independent with $v(b'), b' \in \pi_2$. $\dim(V)$ is at least $N(\pi_2) + 1, \dim(A_{\pi_1} \cap A_{\pi_2}) < \dim(A_{\pi_2})$ $\qquad\square$

Proof of theorem 3 and theorem 4

Proof. Given the condition that $\alpha_k = 1, \forall k$ and $\beta_b = \sum_{k \in b} \alpha_k$, recall $p(A_\pi | z^1, z^2) = \sum_{\pi' \in \mathrm{RF}(\pi)} w(z^1, z^2, \pi')$ and $w(z^1, z^2, \pi) = \frac{1}{c'} \prod_{b \in \pi} \frac{\Gamma(\beta_b + t_b^1 + t_b^2)}{\Gamma(\beta_b + t_b^1)\Gamma(\beta_b + t_b^2)}$

Assuming there are K subgroups, since n_1 and n_2 goes to infinite at same rate, for simplicity we assume $n = \sum_{i=1}^{K} z_i^1 = \sum_{i=1}^{K} z_i^2$, $z^1 \sim \mathrm{multinomial}(\phi), z^2 \sim \mathrm{multinomial}(\psi)$ and $t_b^1 = \sum_{i \in b} z_i^1$ and $t_b^2 = \sum_{i \in b} z_i^2$, so $t_b^1 \sim \mathrm{binomial}\,(n, \Phi_b)$ and $t_b^2 \sim \mathrm{binomial}\,(n, \Psi_b)$, where $\Phi_b = \sum_{i \in b} \phi_i$ and $\Psi_b = \sum_{i \in b} \psi_i$. Let $f(n, b) = \frac{\Gamma(\beta_b + t_b^1 + t_b^2)}{\Gamma(\beta_b + t_b^1)\Gamma(\beta_b + t_b^2)}$, then

$$w(z^1, z^2, \pi) \propto \prod_{b \in \pi} f(n, b)$$

$\log f(n, b) = \log(\Gamma(\beta_b + t_b^1 + t_b^2))$ - $\log(\Gamma(\beta_b + t_b^1))$ - $\log(\Gamma(\beta_b + t_b^2))$, notice that t_b^1, t_b^2 and β_b are integers, and when x is integer, $\Gamma(x)$ is the factorial of $(x - 1)$. We have $\log f(n, b) = \log((\beta_b + t_b^1 + t_b^2 - 1)!) - \log((\beta_b + t_b^1 - 1)!) - \log((\beta_b + t_b^2 - 1)!)$ and when n is large we could use Stirling's approximation, i.e. $\log(n!) = n\log(n) - n + O(\log(n))$, we have $\log((\beta_b + t_b^1 + t_b^2 - 1)!) - \log((\beta_b + t_b^1 - 1)!) - \log((\beta_b + t_b^2 - 1)!) \approx (\beta_b + t_b^1 + t_b^2 - 1)\log(\beta_b + t_b^1 + t_b^2 - 1) - (\beta_b + t_b^1 - 1)\log(\beta_b + t_b^1 - 1) - (\beta_b + t_b^2 - 1)\log(\beta_b + t_b^2 - 1) + O(\log(n))$.

Plug into $f(n, b)$ we have:

$$\log f(n, b) \approx (\beta_b + t_b^1 - 1)\log(1 + \frac{t_b^2}{\beta_b + t_b^1 - 1}) + (\beta_b + t_b^2 - 1)\log(1 + \frac{t_b^1}{\beta_b + t_b^2 - 1}) + O(\log(n))$$

as $\beta_b\log(\beta_b + t_b^1 + t_b^2 - 1) \sim O(\log(n))$ and by law of large number and slutsky's theorem, $\log(1 + \frac{t_b^2}{\beta_b + t_b^1 - 1}) \to \log(1 + \frac{\Psi_b}{\Phi_b})$, $\log(1 + \frac{t_b^1}{\beta_b + t_b^2 - 1}) \to \log(1 + \frac{\Phi_b}{\Psi_b})$ *a.s.* and $\frac{\log f(n, b)}{n} \to \Phi_b\log(1 + \frac{\Psi_b}{\Phi_b}) + \Psi_b\log(1 + \frac{\Phi_b}{\Psi_b})$ a.s. We have:

$$\frac{\log(\prod_{b \in \pi} f(n, b))}{n} \to \sum_b [\Phi_b\log(1 + \frac{\Psi_b}{\Phi_b}) + \Psi_b\log(1 + \frac{\Phi_b}{\Psi_b})] \quad a.s.$$

To find the maxima (Φ, Ψ), we fix Ψ and let $C = \frac{\log(\prod_{b \in \pi} f(n, b))}{n} + \lambda(\sum_{b \in \pi} \Phi_b - 1)$, we have $\frac{\partial C}{\partial \Phi_b} = \log(1 + \frac{\Psi_b}{\Phi_b}) + \lambda$, stationary point is $\Phi_b = \Psi_b, \forall b$. and for the hessian matrix $\frac{\partial^2 C}{\partial \Phi_b^2} = -\frac{\Psi_b}{\Phi_b^2 + \Phi_b\Psi_b} < 0$ and $\frac{\partial^2 C}{\partial \Phi_b \partial \Phi_{b'}} = 0$, if $b \neq b'$, that is to say the hessian matrix is a diagonal matrix with every diagonal elements to be negative, so it is negative definite, and our objective function is concave. The maxima is the stationary point $\Phi = \Psi$. And when $\Phi = \Psi$, $\frac{\log(\prod_{b \in \pi} f(n, b))}{n} = 2\ln(2)$ a constant not dependent on partition π and Φ. That is to

say if $(\phi, \psi) \in A_{\pi_1} \cap A_{\pi_2}$ and $(\phi, \psi) \notin A_{\pi_3}$. Then we would have $\lim_{n \to \infty} \frac{\log(\prod_{b \in \pi_1} f(n,b))}{n} =$
$\lim_{n \to \infty} \frac{\log(\prod_{b \in \pi_2} f(n,b))}{n}$ and $\lim_{n \to \infty} [\frac{\ln(\prod_{b \in \pi_1} f(n,b))}{n} - \frac{\log(\prod_{b \in \pi_3} f(n,b))}{n}] = c > 0$, which implies:

$$\text{(A)} \qquad\qquad \frac{w(z^1, z^2, \pi_3)}{w(z^1, z^2, \pi_1)} \to 0 \quad a.s.$$

To investigate the limit of $\frac{w(z^1, z^2, \pi_1)}{w(z^1, z^2, \pi_2)}$, We use inequalities that $\sqrt{2\pi} n^{n+\frac{1}{2}} e^{-n} \leq n! \leq en^{n+\frac{1}{2}} e^{-n}$ holds for all nonnegative integers n. Plug in $f(n, b)$, we have:

$$\text{(1)} \qquad \beta_b + \log\sqrt{2\pi} - 3 + g(n, b) \leq f(n, b) \leq \beta_b - 2\log\sqrt{2\pi} + g(n, b)$$

$$g(n,b) = (\beta_b + t_b^1 - \frac{1}{2})\log(1 + \frac{t_b^2}{\beta_b + t_b^1 - 1}) + (\beta_b + t_b^2 - \frac{1}{2})\log(1 + \frac{t_b^1}{\beta_b + t_b^2 - 1}) - (\beta_b - \frac{1}{2})\log(\beta_b + t_b^1 + t_b^2 - 1)$$

Based on inequalities (1), $\sum_{b \in \pi} f(n, b)$ only differ with $\sum_{b \in \pi} g(n, b)$ by a constant. By Taylor's expansion $\log(1 + x) = \log 2 + \frac{1}{2}(x - 1) + O((x - 1)^2)$, we have $\log(1 + \frac{t_b^2}{\beta_b + t_b^1 - 1}) = \log 2 + \frac{1}{2}(\frac{t_b^1 - t_b^2 + 1 - \beta_b}{\beta_b + t_b^1 - 1}) + O_p((\frac{t_b^1 - t_b^2 + 1 - \beta_b}{\beta_b + t_b^1 - 1})^2)$ and under condition $\Phi_b = \Psi_b$, $\frac{(t_b^1 - t_b^2 + 1 - \beta_b)^2}{\beta_b + t_b^1 - 1}$ is $O_p(1)$. Plug in $g(n, b)$

$$g(n, b) = \log 2 * t_b^1 + \log 2 * t_b^2 - (\beta_b - \frac{1}{2})\log(\beta_b + t_b^1 + t_b^2 - 1) + O_p(1)$$

and sum up

$$\text{(2)} \qquad \sum_{b \in \pi} g(n, b) = 2n\log 2 - \sum_{b \in \pi}(\beta_b - \frac{1}{2})\log(\beta_b + t_b^1 + t_b^2 - 1) + O_p(1)$$

Notice that when two partition π_1, π_2 have same number of blocks b and $\Phi_b = \Psi_b$, $\forall b \in \pi_1 \cup \pi_2$,

$$\sum_{b \in \pi_1} g(n, b) - \sum_{b' \in \pi_2} g(n, b') = \sum_{b' \in \pi_2}(\beta'_b - \frac{1}{2})\log(\beta'_b + t_{b'}^1 + t_{b'}^2 - 1) - \sum_{b \in \pi_1}(\beta_b - \frac{1}{2})\log(\beta_b + t_b^1 + t_b^2 - 1) + O_p(1)$$

$$= \sum_{b' \in \pi_2}(\beta_{b'} - \frac{1}{2})\log(\frac{\beta'_b + t_{b'}^1 + t_{b'}^2 - 1}{n}) - \sum_{b \in \pi_1}(\beta_b - \frac{1}{2})\log(\frac{\beta_b + t_b^1 + t_b^2 - 1}{n})$$

$$+ \sum_{b' \in \pi_2 - \frac{1}{2}}(\beta_{b'} - \frac{1}{2})\log(n) - \sum_{b \in \pi_1 - \frac{1}{2}}(\beta_b - \frac{1}{2})\log(n) + O_p(1)$$

$$= O_p(1) + \sum_{b \in \pi_1}\frac{1}{2}\log(n) - \sum_{b' \in \pi_2}\frac{1}{2}\log(n)$$

$$= O_p(1)$$

When π_1 and π_2 have same number of blocks,

(B)
$$\frac{J(z^1, z^2, \pi_1)}{J(z^1, z^2, \pi_2)} \to O_p(1) \quad a.s.$$

When π_1 have less blocks than π_2, $\sum_{b' \in \pi_2} g(n, b') - \sum_{b \in \pi_1} g(n, b) = O_p(\log(n))$

(C)
$$\frac{J(z^1, z^2, \pi_1)}{J(z^1, z^2, \pi_2)} \to 0 \quad a.s.$$

$\square$

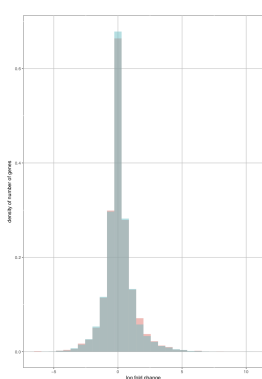we examine log fold change of mean expression across conditions
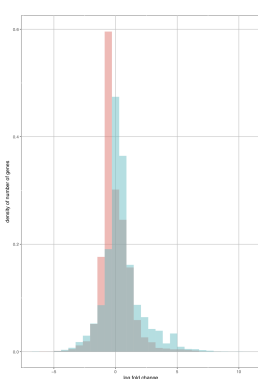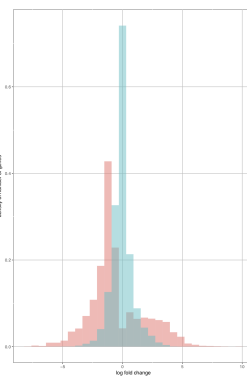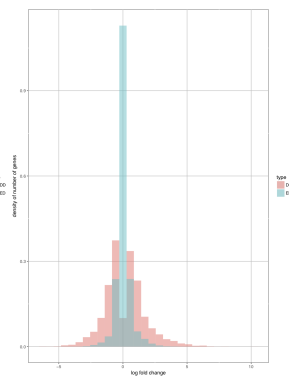

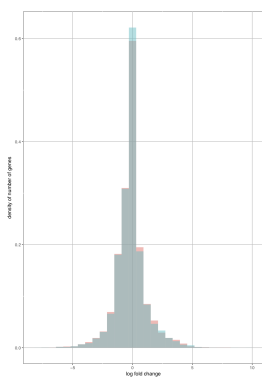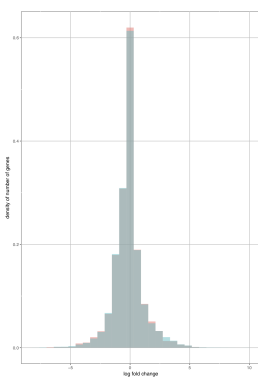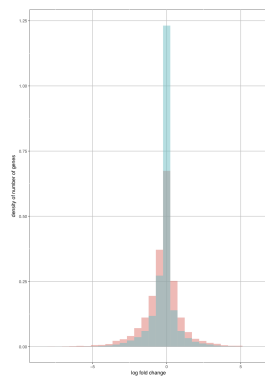FIGURE 14. MAST

FIGURE 15. scDD

FIGURE 16. scD-Dboost

FIGURE 17. DE-Seq2

FIGURE 18. MAST

FIGURE 19. scDD
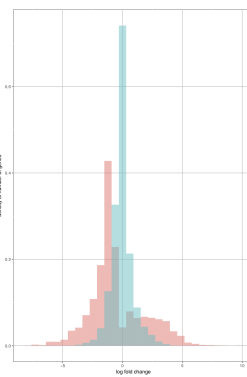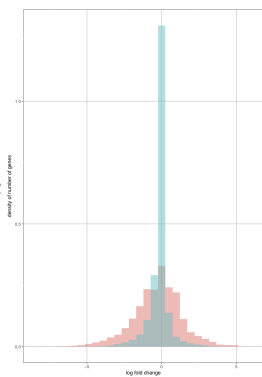

FIGURE 20. scD-Dboost
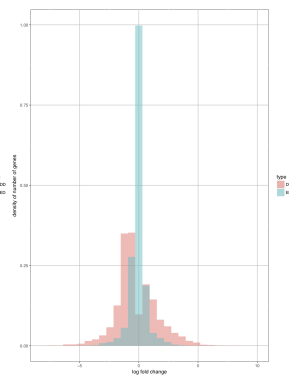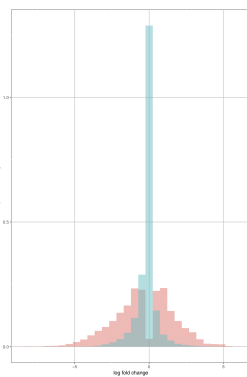

FIGURE 21. DE-Seq2
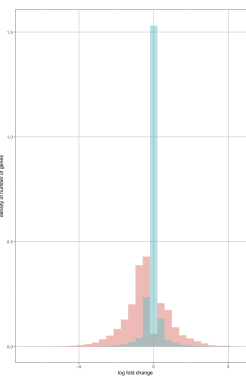
FIGURE 22. MAST

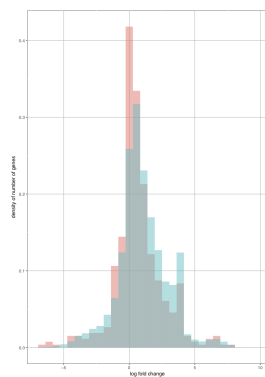FIGURE 23. scDD
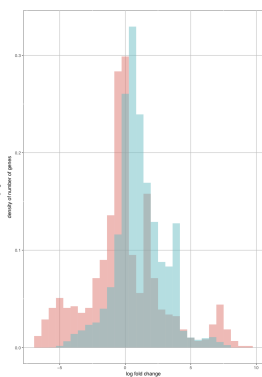

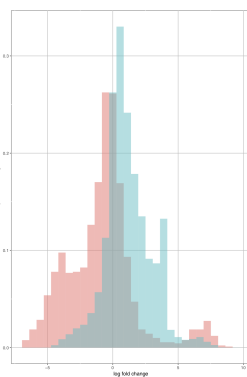FIGURE 24. scD-Dboost

FIGURE 25. DE-Seq2
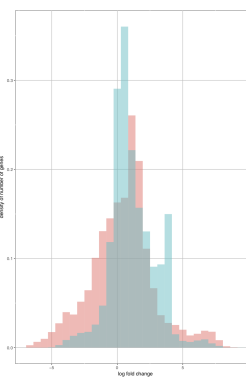

FIGURE 26. MAST

FIGURE 27. scDD

FIGURE 28. scD-Dboost

FIGURE 29. DE-Seq2

REFERENCES

[1] T. Nawy, "Single-cell sequencing," *Nature Methods*, vol. 11, pp. 18 EP –, 12 2013. [Online]. Available: http://dx.doi.org/10.1038/nmeth.2771

[2] R. Bacher and C. Kendziorski, "Design and computational analysis of single-cell rna-sequencing experiments," *Genome Biology*, vol. 17, no. 1, p. 63, 2016. [Online]. Available: https://doi.org/10.1186/s13059-016-0927-y

[3] V. Y. Kiselev, K. Kirschner, M. T. Schaub, T. Andrews, A. Yiu, T. Chandra, K. N. Natarajan, W. Reik, M. Barahona, A. R. Green, and M. Hemberg, "Sc3: consensus clustering of single-cell rna-seq data," *Nature Methods*, vol. 14, pp. 483 EP –, 03 2017. [Online]. Available: http://dx.doi.org/10.1038/nmeth.4236

[4] P. Lin, M. Troup, and J. W. K. Ho, "Cidr: Ultrafast and accurate clustering through imputation for single-cell rna-seq data," *Genome Biology*, vol. 18, no. 1, p. 59, 2017. [Online]. Available: https://doi.org/10.1186/s13059-017-1188-0

[5] E. Pierson and C. Yau, "Zifa: Dimensionality reduction for zero-inflated single-cell gene expression analysis," *Genome Biology*, vol. 16, no. 1, p. 241, 2015. [Online]. Available: https://doi.org/10.1186/s13059-015-0805-z

[6] G. Finak, A. McDavid, M. Yajima, J. Deng, V. Gersuk, A. K. Shalek, C. K. Slichter, H. W. Miller, M. J. McElrath, M. Prlic, P. S. Linsley, and R. Gottardo, "Mast: a flexible statistical framework for assessing transcriptional changes and characterizing heterogeneity in single-cell rna sequencing data," *Genome Biology*, vol. 16, no. 1, p. 278, 2015. [Online]. Available: https://doi.org/10.1186/s13059-015-0844-5

[7] M. I. Love, W. Huber, and S. Anders, "Moderated estimation of fold change and dispersion for rna-seq data with deseq2," *Genome Biology*, vol. 15, no. 12, p. 550, 2014. [Online]. Available: https://doi.org/10.1186/s13059-014-0550-8

[8] K. D. Korthauer, L.-F. Chu, M. A. Newton, Y. Li, J. Thomson, R. Stewart, and C. Kendziorski, "A statistical approach for identifying differential distributions in single-cell rna-seq experiments," *Genome Biology*, vol. 17, no. 1, p. 222, 2016. [Online]. Available: https://doi.org/10.1186/s13059-016-1077-y

[9] D. B. Dahl, "Modal clustering in a class of product partition models," *Bayesian Anal.*, vol. 4, no. 2, pp. 243–264, 06 2009. [Online]. Available: https://doi.org/10.1214/09-BA409

[10] A. Strehl and J. Ghosh, "Cluster ensembles — a knowledge reuse framework for combining multiple partitions," *J. Mach. Learn. Res.*, vol. 3, pp. 583–617, Mar. 2003. [Online]. Available: https://doi.org/10.1162/153244303321897735

[11] B. Dickey J., Lientz, "The weighted likelihood ratio, sharp hypotheses, and the order of a markov chain." *Ann. Math. Statist.*, vol. 41, no. 1, p. 214, 1970. [Online]. Available: https://projecteuclid.org/euclid.aoms/1177697203

[12] U. Wagner and A. Taudes, "A multivariate polya model of brand choice and purchase incidence," *Marketing Science*, vol. 5, no. 3, pp. 219–244, Aug. 1986. [Online]. Available: http://dx.doi.org/10.1287/mksc.5.3.219

[13] H. I. Weisberg, "Bayesian comparison of two ordered multinomial populations," *Biometrics*, vol. 28, no. 3, pp. 859–867, 1972. [Online]. Available:

http://www.jstor.org/stable/2528768

[14] L. Zappia, B. Phipson, and A. Oshlack, "Splatter: simulation of single-cell rna sequencing data," *Genome Biology*, vol. 18, no. 1, p. 174, 2017. [Online]. Available: https://doi.org/10.1186/s13059-017-1305-0

[15] R. Bacher, L.-F. Chu, N. Leng, A. P. Gasch, J. A. Thomson, R. M. Stewart, M. Newton, and C. Kendziorski, "Scnorm: robust normalization of single-cell rna-seq data," *Nature Methods*, vol. 14, pp. 584 EP –, 04 2017. [Online]. Available: http://dx.doi.org/10.1038/nmeth.4263

[16] N. Leng, J. A. Dawson, J. A. Thomson, V. Ruotti, A. I. Rissman, B. M. G. Smits, J. D. Haag, M. N. Gould, R. M. Stewart, and C. Kendziorski, "Ebseq: an empirical bayes hierarchical model for inference in rna-seq experiments," *Bioinformatics*, vol. 29, no. 8, pp. 1035–1043, 2013. [Online]. Available: + http://dx.doi.org/10.1093/bioinformatics/btt087

[17] C. Soneson and M. D. Robinson, "Bias, robustness and scalability in differential expression analysis of single-cell rna-seq data," *bioRxiv*, 2017. [Online]. Available: https://www.biorxiv.org/content/early/2017/05/28/143289

[18] Q. Deng, D. Ramsköld, B. Reinius, and R. Sandberg, "Single-cell rna-seq reveals dynamic, random monoallelic gene expression in mammalian cells," *Science*, vol. 343, no. 6167, pp. 193–196, 2014. [Online]. Available: http://science.sciencemag.org/content/343/6167/193

[19] A. K. Shalek, R. Satija, J. Shuga, J. J. Trombetta, D. Gennert, D. Lu, P. Chen, R. S. Gertner, J. T. Gaublomme, N. Yosef, S. Schwartz, B. Fowler, S. Weaver, J. Wang, X. Wang, R. Ding, R. Raychowdhury, N. Friedman, N. Hacohen, H. Park, A. P. May, and A. Regev, "Single-cell rna-seq reveals dynamic paracrine control of cellular variation," *Nature*, vol. 510, pp. 363 EP –, 06 2014. [Online]. Available: http://dx.doi.org/10.1038/nature13437

[20] R. M. Kumar, P. Cahan, A. K. Shalek, R. Satija, A. Jay DaleyKeyser, H. Li, J. Zhang, K. Pardee, D. Gennert, J. J. Trombetta, T. C. Ferrante, A. Regev, G. Q. Daley, and J. J. Collins, "Deconstructing transcriptional heterogeneity in pluripotent stem cells," *Nature*, vol. 516, pp. 56 EP –, 12 2014. [Online]. Available: http://dx.doi.org/10.1038/nature13920

[21] I. Engel, G. Seumois, L. Chavez, D. Samaniego-Castruita, B. White, A. Chawla, D. Mock, P. Vijayanand, and M. Kronenberg, "Innate-like functions of natural killer t cell subsets result from highly divergent gene programs," *Nature Immunology*, vol. 17, pp. 728 EP –, 04 2016. [Online]. Available: http://dx.doi.org/10.1038/ni.3437

[22] F. Buettner, K. N. Natarajan, F. P. Casale, V. Proserpio, A. Scialdone, F. J. Theis, S. A. Teichmann, J. C. Marioni, and O. Stegle, "Computational analysis of cell-to-cell heterogeneity in single-cell rna-sequencing data reveals hidden subpopulations of cells," *Nature Biotechnology*, vol. 33, pp. 155 EP –, 01 2015. [Online]. Available: http://dx.doi.org/10.1038/nbt.3102

[23] F. Guo, L. Yan, H. Guo, L. Li, B. Hu, Y. Zhao, J. Yong, Y. Hu, X. Wang, Y. Wei, W. Wang, R. Li, J. Yan, X. Zhi, Y. Zhang, H. Jin, W. Zhang, Y. Hou, P. Zhu, J. Li, L. Zhang, S. Liu, Y. Ren, X. Zhu, L. Wen, Y. Q. Gao, F. Tang, and

J. Qiao, "The transcriptome and dna methylome landscapes of human primordial germ cells," *Cell*, vol. 161, no. 6, pp. 1437–1452, 2017/12/05. [Online]. Available: http://dx.doi.org/10.1016/j.cell.2015.05.015

[24] B. Tasic, V. Menon, T. N. Nguyen, T. K. Kim, T. Jarsky, Z. Yao, B. Levi, L. T. Gray, S. A. Sorensen, T. Dolbeare, D. Bertagnolli, J. Goldy, N. Shapovalova, S. Parry, C. Lee, K. Smith, A. Bernard, L. Madisen, S. M. Sunkin, M. Hawrylycz, C. Koch, and H. Zeng, "Adult mouse cortical cell taxonomy revealed by single cell transcriptomics," *Nature Neuroscience*, vol. 19, pp. 335 EP –, 01 2016. [Online]. Available: http://dx.doi.org/10.1038/nn.4216

[25] L.-F. Chu, N. Leng, J. Zhang, Z. Hou, D. Mamott, D. T. Vereide, J. Choi, C. Kendziorski, R. Stewart, and J. A. Thomson, "Single-cell rna-seq reveals novel regulators of human embryonic stem cell differentiation to definitive endoderm," *Genome Biology*, vol. 17, no. 1, p. 173, 2016. [Online]. Available: https://doi.org/10.1186/s13059-016-1033-x

[26] N. Leng, L.-F. Chu, C. Barry, Y. Li, J. Choi, X. Li, P. Jiang, R. M. Stewart, J. A. Thomson, and C. Kendziorski, "Oscope identifies oscillatory genes in unsynchronized single-cell rna-seq experiments," *Nature Methods*, vol. 12, pp. 947 EP –, 08 2015. [Online]. Available: http://dx.doi.org/10.1038/nmeth.3549

[27] M. Delmans and M. Hemberg, "Discrete distributional differential expression (d3e) - a tool for gene expression analysis of single-cell rna-seq data," *BMC Bioinformatics*, vol. 17, no. 1, p. 110, 2016. [Online]. Available: https://doi.org/10.1186/s12859-016-0944-6

E-mail address: `newton@biostat.wisc.edu`